Freestanding, Highly Flexible, Large Area, Nanoporous Alumina Membranes with Complete Through-Hole Pore Morphology

Jörg J. Schneider,*[a] Jörg Engstler,[a] Karl P. Budna,[a,b] Christian Teichert,[c] and Steffen Franzka[d]

Keywords: Alumina / Electrochemistry / Porous template / Oxidation

Electrochemical anodic oxidation of aluminium metal sheets leads to the formation of compact and dense, but highly porous alumina surfaces on top of the anode. The alumina surfaces obtained by anodic oxidation can be detached from the bare metal by using a voltage detachment procedure, without employing chemical etching techniques. This procedure leads to large area porous alumina membranes with closed backsides. Prestructuring of the aluminium base metal leads to ordered pore regions at anodisation voltages of 25, 40 and 50 V, resulting in porous alumina membranes with pore diameters of 33, 40 and 72 nm. The careful opening of the backside alumina membranes can be realised by acid treatment leading to highly flexible large area porous alumina membranes with complete through-hole pore morphology. The backside pore-opening process realised by chemical etching is strongly dependent on time and acid concentration and is best monitored routinely by microscopy techniques in order to gain control over the process.

Introduction

Over the last few years mesoporous alumina has attracted much scientific interest in materials chemistry because of its compact and highly ordered porous structure.[1] These features, in combination with the possibility to vary the pore size of the individual alumina pores between 10 and 300 nm, as well as its high temperature and chemical resistance, makes this material attractive as a template material for the synthesis of one-dimensional ordered nanoscaled functional materials such as wires, tubes, fibres and particles.[2] The thickness of the porous alumina membrane which determines the pore length as well as the pore diameter is controlled by the electrochemical synthesis conditions of the anodic oxidation process. Aside from the electrochemical parameters, a dependence of its properties on temperature, pH, time of the process, as well as the aluminium metal surface conditions is observed. It is highly desirable to have as much experimental control as possible over the complex alumina formation process, because the alumina pore morphology controls the morphology of the templated guest materials incorporated within the pores. Therefore it is necessary to control the synthetic anodisation process as well as the detachment and pore conditioning process in its crucial parameters: (a) pore size, (b) membrane thickness, (c) regular arrangement of the pores, (d) detachment of the *p*orous *a*lumina *ox*ide (PAOX) membrane from the aluminium base metal and (e) generation of a complete through-hole pore morphology of the PAOX membrane. Point (e) is especially important for employing PAOX membranes in controlled gas phase processes, for example in a chemical vapour deposition nanoreactor in which gaseous species are transported through or reacted within the PAOX membrane. Examples in this area are the formation of carbon nanotubes[3] or polymer fibres derived from [2.2] paracyclophane[4] as well as catalytic gas phase hydrogenation and CO oxidation reaction.[5]

Herein we present our investigations on the synthesis of alumina membranes with regular hexagonal pore order. These membranes are produced at 25, 40 and 50 V anodisation voltage giving rise to 33, 40 and 72 nm diameter pores. To the best of our knowledge and despite the intensive use of the unique pore system of PAOX membranes in synthetic materials chemistry, no detailed studies dealing with backside pore opening of PAOX membranes has been reported. One goal is to establish reliable experimental protocols for PAOX alumina backside pore opening. This is necessary in order to employ PAOX membranes on a broader basis, for example as a nanoporous template platform in synthetic as well as catalytic gas phase processes. A qualitative model of the stepwise pore opening is developed herein which offers for the first time an experimental verifi-

[a] Fachbereich Chemie, Eduard-Zintl-Institut für Anorganische und Physikalische Chemie, Technische Universität Darmstadt, Petersenstraße 18, 64287 Darmstadt, Germany
Fax: +49-06151-16-3470
E-mail: joerg.schneider@ac.chemie.tu-darmstadt.de
[b] Current address: Institut für Metallkunde und Werkstoffprüfung, Montanuniversität Leoben, 8700 Leoben, Austria
[c] Institut für Physik, Montanuniversität Leoben, 8700 Leoben, Austria
[d] Fachbereich Chemie, Institut für Physikalische Chemie, Universität Duisburg-Essen, 45117 Essen, Germany

cation of the dissolution processes of the different dense alumina compositions which constitute the PAOX pore walls. This procedure allows the experimental realisation of freestanding, large area PAOX membranes with enhanced mechanical flexibility (area size of several 10 cm^2) and complete through-hole pore morphology.

General Features of Porous Anodic Alumina

Figure 1 represents a schematic top view on the surface of the open pore side of a PAOX membrane. The membrane is constructed of individual alumina cells with hexagonal cell shape. In the centre of these hexagonal cells are uniform uniaxially rounded pores. The diameter of the PAOX cells as well as the diameter of the PAOX pores is directly proportional to the applied anodisation voltage.[6] The pore walls consist of two different types of alumina.[7] On the one hand is a relatively pure anion-free dense alumina which makes up the hexagonal body of the cell. This material is not in direct contact with the pore itself. On the other hand, in the inner cell region is an electrolyte-contaminated less dense alumina, which forms the pore wall. Figure 1 (part a) shows a cross-section of the PAOX membrane with the unidirectional pore arrangement. At the bottom the pores are separated from the aluminium metal base by the barrier layer, which seals the PAOX membrane on one side. To obtain a total through-hole pore morphology (i) the PAOX membrane has to be detached from the aluminium metal base and (ii) a pore opening process has to be employed which dissolves the barrier layer and forms a uniform pore diameter *without* destroying the overall porous backside structure. Steps (i) and (ii) have to be applied consecutively in two independent processes.

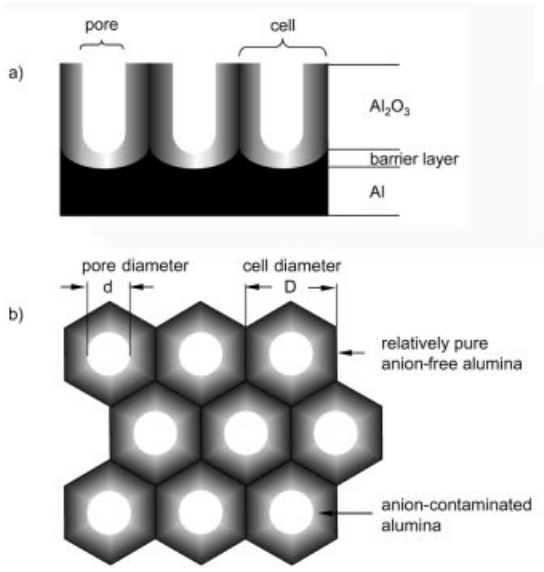

Figure 1. Schematic view of the characteristics of an idealised PAOX membrane pore geometry. (a) Schematic of the cross section of the unidirectional pore arrangement of a PAOX membrane. The pores are sealed on one side by the convex shaped barrier layer, which forms the connection of the PAOX membrane to the aluminium metal base. (b) Top view of the surface showing the hexagonal cells with the central through-hole pores. The alumina consists of two different types: (i) relatively pure dense alumina which constitutes the outer cell region cell and (ii) anion-contaminated, less dense alumina, which forms the surrounding through-hole pore material which is in direct contact with the inner pore. This different material composition is schematically shown by the greyish colour graduation.

Results and Discussion

Our first experimental step in the synthesis of alumina membranes is the high temperature annealing of commercial aluminium sheets at 400 °C. This procedure relaxes the surface of the aluminium base metal from defects.[8] Figure 2 (part a) shows an SEM picture of as-received aluminium (99.93%, PURALUX®). The general roughness of the surface as measured by AFM is 47 nm. Part b of Figure 2 shows an SEM picture of the same aluminium sheet after heat treatment under air (400 °C) for 1 h. Its roughness has increased. The general roughness of the heat-treated aluminium is about 100 nm as compared to 47 nm before this treatment. This difference can be explained by a thermal expansion of the aluminium sheet during the heat treatment followed by subsequent contraction of the metal surface while cooling down to room temperature.[9] This relaxes stresses within the surface, but on the other hand results in a folding of the surface which increases the overall roughness in comparison to the untreated material.

To remove this surface roughness the heat-treated metal specimen is electropolished in a solution of perchloric acid in ethanol.[10] Electropolishing is used in deburr processes

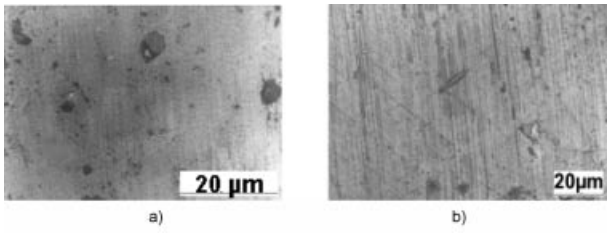

Figure 2. SEM pictures of (a) aluminium PURALUX® as received, (b) PURALUX® surface after heat treatment of 450 °C for 1 h. The roughness of the surface has increased.

of metals, where cutting edges of metals are flattened. This treatment removes the induced roughness of the Al metal sheet surface by chemical etching. The roughness of the aluminium surface after electropolishing is about 29 nm as detected by AFM (part a in Figure 3). However, what is most important here for the alumina surface is that the electropolishing procedure pretextures the metallic surface on a nanoscale [Figure 3, parts a (AFM) and b (SEM)]. This pretexturing is dependent on the applied voltage. The diameter of the concave spots on the electropolished aluminium surface (SEM, Figure 3, part b) is about 55 nm at 40 V. A direct connection exists between the electropolishing conditions employed and the formation of the PAOX membranes by the follow-up anodic oxidation process (see below and upcoming section on PAOX membrane formation).

Nevertheless, other recent reports on the formation of PAOX membranes claim no significant effect of electropolishing on the prestructuring of the aluminium metal surface.[11]

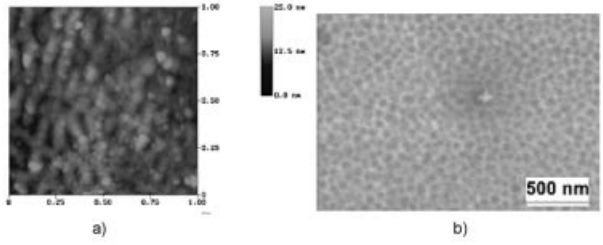

Figure 3. (a) AFM picture of an electropolished aluminium surface (1×1 μm^2 scan, height bar 0–25 nm). The roughness of the surface is 30 nm. (b) Concave structures (diameter 60 nm) on the top of the surface are visible by SEM. The diameter of the concave part is in the range of 60 nm.

Figure 4 shows an SEM of an aluminium surface which was first electropolished (see Exp. Section) followed by long-term anodic oxidation for 24 h, followed by detachment of the thus formed alumina membrane from the aluminium metal base by reversing the initially applied anodisation voltage (see Exp. Section).[12] This procedure leaves the aluminium metal base with a characteristic starting pore geometry on top (Figure 4). The diameter of the concave hollows on the metal surface is 80 nm, which is in fair agreement with the theory of voltage versus cell/pore size relationship of PAOX films. For an anodic oxidation voltage of 40 V, as in the present experiments, values of 51.6 nm for the pore diameter and 110.8 nm for the overall cell diameter are expected.[6] The mean diameter of the experimentally observed concave hollow structures (80 nm) on the aluminium surface is between these two values.

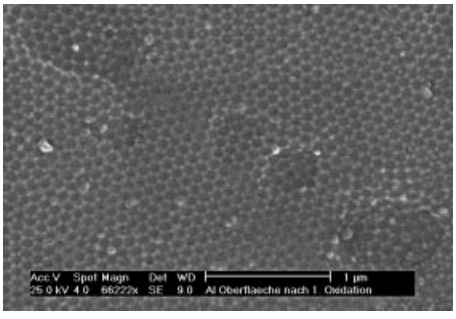

Figure 4. SEM picture of an aluminium surface after first anodisation and detachment of the resulting alumina membrane.

These results show that the different steps of pretreatment of the aluminium base metal have an enormous effect on the structure of the surface. It is interesting to note that the concave oxidic hollows on the underlying aluminium metal base generated by detachment of the PAOX membrane may serve as future template structures for depositing ordered nanodots of equivalent dot size.

Preparation of Freestanding PAOX Membranes with Through-Hole Morphology

After having studied the initial steps of porous oxide formation, we investigated the formation of PAOX membranes with hexagonally ordered pores at anodisation voltages of 25, 40 and 50 V in more detail. For pretexturing the electropolished aluminium surface we carried out the above-described process involving electropolishing followed by an anodic anodisation for 24 h, followed by detachment of the resulting membrane from the aluminium backside by reverse voltage technique (see Exp. Section). This procedure results in aluminium metal sheets with hexagonal textured structures on top (Figure 4). To obtain PAOX membranes from such prestructured metal surfaces we then performed a final anodisation step under the same electrolysis conditions as before with such a prestructured aluminium surface. The complete procedure was carried out for PAOX membranes under anodisation conditions of 40, 50 and finally 20 V.

40-V PAOX Membranes from Prestructured Aluminium Surfaces

Prestructured aluminium metal sheets (see above) were finally anodised for 20 h/10 °C/40 V anodisation voltage (see experimental). The resulting PAOX membrane was then detached from the aluminium base by reversing the voltage (Figure 5). We have optimised this technique and found that membrane detachment by the voltage reversal has significant advantages over chemical detachment methods using $HgCl_2$ or $CuBr_2$ often employed to obtain freestanding PAOX membranes. Detachment by careful voltage reversal allows production of up to several square centimetres of sized flexible PAOX membranes which may find use in future large area template applications (Figure 6).

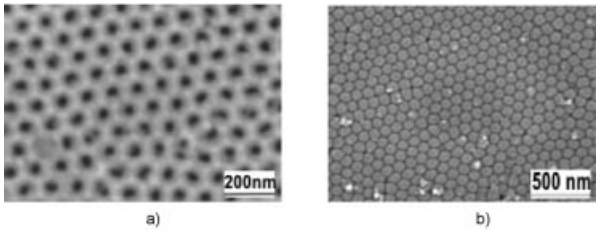

Figure 5. SEM pictures of a detached PAOX membrane prepared in a second anodisation step at 40 V. (a) Front side with hexagonally ordered open pores, (b) rear side with closed hexagonally ordered pores.

In Figure 5 the hexagonally ordered open pores of the PAOX membrane can be seen. The uniform diameter of the pores is 36 nm (±2 nm) and the cell diameter is 105 nm (±4 nm). It is known that the pore walls of PAOX membranes contain varying amounts of electrolyte.[7,13,14] The contrast-rich region of the SEM picture, next to the middle of the neighbouring pores, represents electrolyte-free dense alumina (see Figure 1). The less contrast-rich part of the inner pore region corresponds to the electrolyte-containing

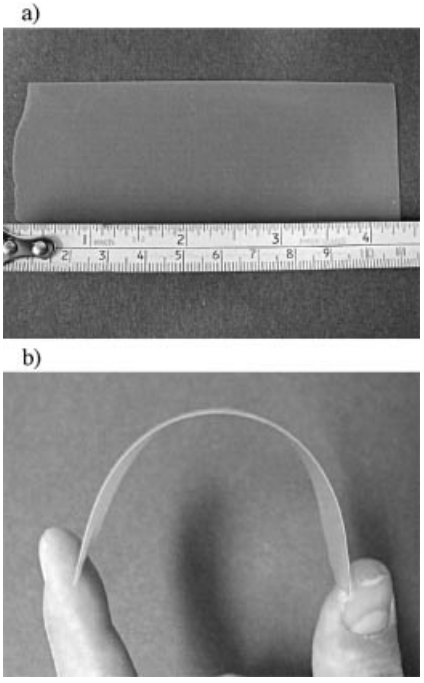

Figure 6. (a) Photo of a freestanding PAOX membrane (size about 40 cm^2). (b) Same sized PAOX membrane under manual mechanical torsion.

part of alumina. Their distinction in the SEM is due to the scattering behaviour of the electron beam for different dense materials. Figure 5b shows the rear side of a detached PAOX membrane. The hexagonally arranged pores are closed because of the presence of the barrier layer. Figure 7 (pos. 1, pos. 2) shows regions in which highly ordered domains are separated from unordered domains by different unordered boundary pore arrangements, for example, a flowerlike arrangement (Figure 7, pos. 1) and a linear arrangement of pores (Figure 7, pos. 2). We have observed such morphologies separating well ordered, hexagonally arranged pore regions from each by lower ordered regions throughout the whole PAOX membrane structure over cm^2 large areas in several independent experiments. The pore formation process in PAOX membranes has been studied theoretically by applying the mathematical theory of Voronoi.[14,15] Similar disordered pore structures are expected

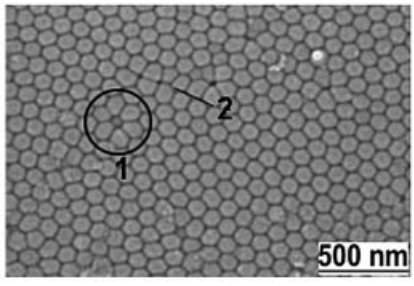

Figure 7. SEM of a backside of a detached PAOX membrane showing different ordered domains. Several kinds of disorder can be observed at the boundaries of the domains. Defects labelled with 1 have a flowerlike structure, and those labelled 2 display a linear structure.

by the theoretical model reported therein, and are also found experimentally by others.[15] This inherent and characteristic domain disorder of PAOX membranes can be overcome to a significant extent by using a prestructured alumina metal base which is available, for example, by embossing techniques using mechanically hard master stamps (produced e.g. by e-beam lithography), as has been shown by Masuda et al. for the first time.[16]

Figure 8 shows a cross-section of a typical PAOX membrane generated at 40 V exhibiting an all through parallel pore morphology. The nearly perfect parallel pore structure running orthogonal to the PAOX membrane surface is evident.

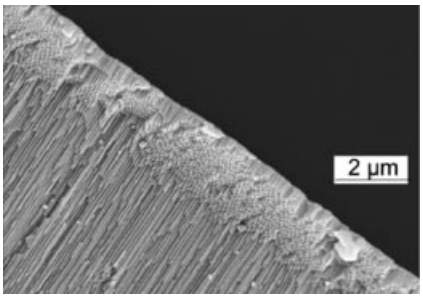

Figure 8. SEM of a cross-section of a detached PAOX membrane generated at 40 V. The pore channels are nearly perfectly parallel and orthogonally aligned to the surface which is seen partly in the foreground of the image. The channels are running from the top to the bottom of the image.

50-V PAOX Membrane from Prestructured Aluminium Surfaces

Figure 9 (parts a, b) show the front side of such a membrane. A hexagonal order of pores in μm^2-sized domains can be seen. The pore diameter is 57 nm (±4 nm) and the cell diameter is 114 nm (±4 nm), both corresponding to the values expected theoretically, which are 64.5 nm for the pore diameter and 138.5 nm for the cell diameter.[6] Part c of Figure 9 depicts the closed backside of a PAOX membrane detached from the aluminium metal base by the voltage reversal technique. The hexagonal ordering of the pores is again nearly perfect. Figure 9 (part d) shows the massive parallel pore arrangement of such a PAOX channel system.

We also routinely generated hexagonally ordered alumina membranes at 25-V anodisation voltage with the same morphological characteristics as discussed for the 40- and 50-V membranes (SEM, AFM topological characterisation not shown). Their pore diameter is 36 nm (±3 nm) and the cell diameter 64 nm (±2 nm), both in good agreement with the theoretical values of 32 and 69 nm for the cell and pore diameters, respectively.

Controlled Dissolution Studies of the Barrier Layer from Freestanding PAOX Membranes

For detachment of the alumina membrane after their synthesis we generally use the reversing voltage technique

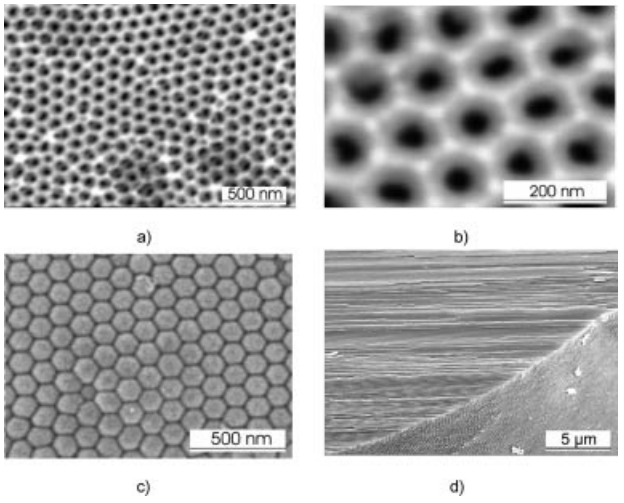

Figure 9. SEM of hexagonally ordered pores of a detached PAOX membrane generated at 50 V with complete through-hole morphology. (a) Front side of a PAOX membrane generated at 50 V with hexagonally ordered open pores; (b) as (a), but higher magnification; (c) back side of a PAOX membrane (50 V) with closed barrier layer; (d) cross-section of the same membrane with parallel pore arrangement.

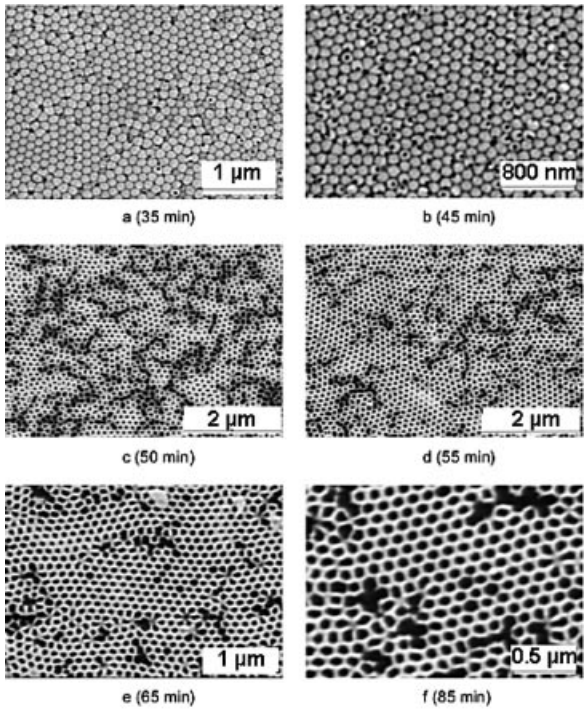

Figure 10. SEM images of the barrier layer of a PAOX membrane (50 V) at different intervals of backside pore opening (5% H_3PO_4). After 45 min of acid treatment (9a and 10b) the majority of the pores are still closed. After 50 min (c) pores are fully opened and pore widening of the inner pores starts to take place. (d) Further etching leads to an increased pore widening and subsequent destruction of the opened alumina membrane backside. This occurs predominantly in areas of hexagonal disorder [e and f (scale bar 200 nm)].

(see before). This results in the formation of a freestanding PAOX membrane with a *single* open pore side. The open pore side represents the initial oxidation front of the electrochemical anodisation process and reflects in its cell size and overall surface structure the unsteady electrolysis conditions present during the beginning of the aluminium oxidation when equilibrium conditions for pore cell formation have not been reached. The closed side of the PAOX membrane, the barrier side, represents the front of the ongoing oxidation process directly attached to the aluminium metal substrate. Therefore the backside typically shows well-arranged pore cells, because electrolysis conditions reach an equilibrium state during the ongoing anodisation.

Time-Dependent Acid Etch of the Barrier Layer

In numerous experiments we have found that the process of pore opening of the backside of PAOX membranes is experimentally the most difficult procedure in obtaining PAOX membranes with a complete through-hole morphology.[16] It depends crucially on the acid strength, and time and type of contact in order to open the closed backside in a controlled and reproducible way. Control over this process by straightforward chemical etching techniques is desirable in order to have access to through-hole open pore geometries with different pore diameters.

To obtain PAOX membranes with a continuous through-hole pore morphology we studied dissolution of the barrier layer over different time intervals. In our experiments we studied hexagonally arranged PAOX membranes that were generated at 50 V and the barrier layer was dissolved with 5% H_3PO_4 (aq.) over time. Figure 10 (parts a–f) show SEM micrographs at different time intervals representing different stages of barrier layer dissolution.

35 min of Acid Treatment

The initial dissolution process starts by producing hole structures in the convex domes of the barrier layer (Figure 10, part a). The location of the holes in the individual pores appear as black dots distributed inhomogeneously over the membrane surface, for example holes can be observed in the centre of one pore, as well at the edges of individual pores. The majority of the backside pore domes, however, are still unaffected after that time interval.

45–55 min of Acid Treatment

After 45 min the number of partially opened backside pore domes has increased significantly (Figure 10, part b). Interestingly the dimensions of the already opened pore domes from the first etch period (35 min) are nearly unaffected. After 50 and 55 min of dissolution (Figure 10, parts c and d) the barrier layer is completely removed and all pores are opened. However different stages of pore opening are detectable after these times. Some pores are opened to such an extent that connecting neighbouring pores are already affected. This effect is observed to a significantly large extent in domain areas where cell disorder is found. Ordered domain areas show a more even pore dissolution characteristic. This effect is even more pronounced after

65 min (Figure 10, part e) and after 85 min (Figure 10, part f) of pore dome dissolution. With ongoing acid treatment, not only are the disordered parts of the membrane dissolved, but the structure of the inner pore walls of the ordered regions also becomes larger. This is due to an ongoing dissolution of alumina from the already opened pores. This process is generally known as pore widening and is caused by the dissolution of the electrolyte-rich inner alumina phase. In Figure 10f the inner alumina phase is nearly completely dissolved, leaving the electrolyte-free outer alumina portion of the pore cell structure, which is not prone to dissolution under these conditions, unaffected.

Based on the results of these dissolution experiments we have developed a scheme illustrating the acid dissolution process of the PAOX membrane backside over time (Figure 11).

The first step of the dissolution process is a slow thinning of the outer electrolyte-free alumina, which represents the top of the barrier layer of the convex dome structures as shown in (a) on the left-hand side of Figure 11. Until dissol-

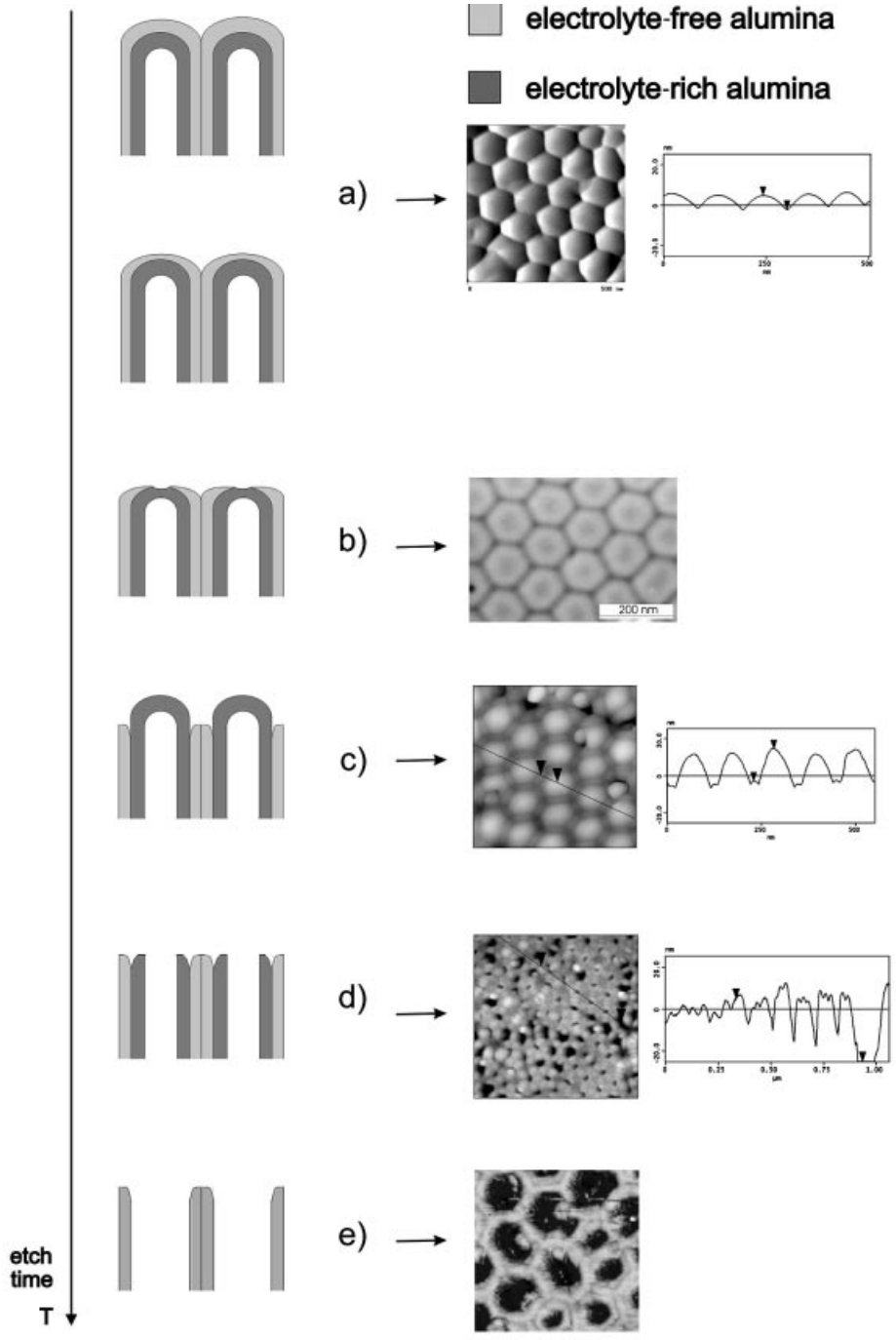

Figure 11. Scheme of the dissolution process leading to a pore opening by acid treatment (see text for details). (a) Line scan 0–500 nm, height bar 0–20 nm; (b) scale bar SEM 200 nm; (c) line scan 0–500 nm, height bar 0–20 nm; (d) line scan 0–1 μm, height bar 0–20 nm.

ution of the alumina dome caps of the backside has progressed significantly, we are not able to detect any significant change in morphology using AFM. After increasing reaction time the dome caps are dissolved to a significant extent, which can be visualised by SEM (Figure 11b). The initial process of dome cap opening needs a significantly longer time compared to the next steps of the overall dissolution process finally leading to the complete opening of the PAOX membrane backside. A rationale for this can be found in the different compositions of the outer and inner alumina compositions of the PAOX cell structure (see Figure 1). The dome caps of the alumina cells are composed of electrolyte-free (Figure 11, light grey region) and electrolyte-contaminated alumina (Figure 11, dark grey region). The former is more resistant towards acidic dissolution than the inner pore walls of the cells. Once the outlying, more dense, electrolyte-free alumina part of the dome caps has been completely dissolved, the overall backside dissolution process leading to complete pore opening proceeds very quickly.

Part c of Figure 11 shows the situation of a strongly dissolved, electrolyte-free alumina dome cap structure. The pore walls are already strongly dissolved in comparison to the still closed underlying dome cap of the electrolyte-containing alumina (see AFM cross-section analysis, Figure 11, part c, right side). The interface region separates two neighbouring, still closed pores in which the electrolyte-free alumina is completely dissolved.

The next step in the dissolution process is the beginning of the complete pore opening which produces the desired through-hole morphology of the PAOX membrane (AFM, Figure 11, part d; right side). Ongoing dissolution opens the pores to a further significant extent (Figure 11, part e). This last dissolution step is the so-called pore-widening step because it enlarges the entrance part of the opened pores over their regular sized dimensions (the 'pore size', see Figure 1) by dissolving interior material from the alumina pores. Obviously the pore-opening model developed here is in good agreement with the dissolution process as it is verified experimentally in Figure 10.

The required times for total pore opening and widening (Figure 11, part e) for 25-, 40- and 50-V PAOX membranes are summarised in Table 1. With increasing pore diameter and barrier-layer thickness, the time for pore opening increases. However, no linear correlation between dissolution time, anodisation voltage and thickness of the barrier layer was found. To obtain reproducible PAOX membrane properties we check the PAOX morphology by routine interval SEM studies to watch the ongoing dissolution process in a stepwise manner. These checks allow simple but efficient control of the pore-opening process and give the possibility of varying pore entrance diameters at will just by stopping the chemical etching process at a certain time. To the best of our knowledge such control over pore entrance diameters in PAOX membranes has only been reported by using grazing angle Ar ion milling[17] of a closed PAOX membrane backside. This technique is able to produce certain degrees of pore openings. However, this is a technique that is not applicable over several cm^2-large PAOX membrane areas as we have reported herein with the time-controlled etching method.

Table 1. Typical time intervals for generation of a PAOX membrane with complete through-hole pore morphology generated from a detached PAOX membrane with closed backside at different anodisation voltages viz. different pore and cell diameters.

Anodisation voltage [V]	Time of acid treatment [min]
25	23
40	75
50	85

Another point of importance for the pore-opening procedure is the occurrence of domain boundaries between ordered pore regions. They represent areas of local disorder in which alumina surrounding these areas is dissolved more quickly than alumina in higher ordered areas. This effect is demonstrated in Figure 12 in which the initial start period of a PAOX backside dissolution process is shown. Dissolution is predominant in areas where disordered structures are present (boundary regions), denoted by dark circles.

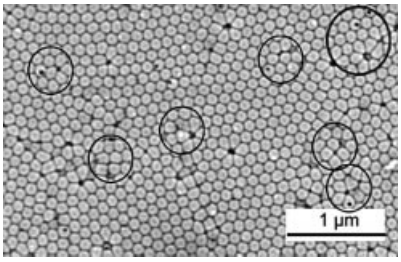

Figure 12. SEM picture of alumina membrane barrier layer at an early stage of backside pore opening. The circles mark positions where pore opening is observed preferentially. This is dominantly α or β to a location of pore disorder.

Conclusion

We have synthesised freestanding, large area sized PAOX membranes with an all through pore arrangement by electrochemical anodic oxidation of aluminium followed by detachment and selective pore opening. We have shown that hexagonally ordered pores over several square µm regions can be obtained at anodisation voltages of 25, 40 and 50 V, resulting in PAOX membranes with pore diameters of 33, 40 and 72 nm.

It has also been shown by AFM and SEM investigations that pretreatment (annealing and electropolishing) of the aluminium metal substrate, especially the applied voltage in the electropolishing step, has a significant influence on the quality and order of the pores of the PAOX membrane. By using the reversing voltage technique for detachment of the prepared alumina membrane, samples with an open pore side and a closed barrier side are obtained. We investigated a time resolved dissolution of the barrier layer with AFM and SEM. Based on these results we have proposed a mechanism for the successive dissolution of the closed pores

with H_3PO_4. This allows access to flexible, freestanding, large area PAOX membranes with ordered pore geometries and completes through-hole pore morphology on a routine experimental basis by straightforward chemical techniques.

Experimental Section

General Information: Aluminium (99.93%, PURALUX Quality) was from AMAG, Ranshofen, Austria. For SEM characterisation the PAOX membranes were sputter coated with gold using a Cressington 108a sputter coater. SEM was carried out with a Zeiss Gemini DSM 982 and AFM was done with a DI Nanoscope IIIa in the tapping mode. Pore and cell diameter measurements of PAOX membranes were made on a statistical basis determining up to 20 structures in different domain areas of the membrane.

Electropolishing of the Aluminium Base Metal: This was performed in a mixture of ethanol and perchloric acid (4:1, vol.-%) at 0 °C. The distance of the aluminium electrodes was fixed at 9 cm. The best results for polishing were obtained with current densities between 0.25 and 0.40 A cm^{-2}. The polishing voltage was the same as for the following anodisation step. After 3 min of polishing the anode was removed while voltage was still on and was rapidly rinsed with water and acetone.

PAOX Sample Preparation (General Preparation Procedure): $10 \times 3 \times 0.13$ cm aluminium base metal sheets were first degreased with acetone and subsequently annealed at 400 °C for one hour. Following the electropolishing of the sample (current density between 7 and 30 mA cm^{-2}) a first anodisation was carried out for 24 h followed by voltage reversal at the same voltage to detach the membrane from the alumina base. Time for detachment varies between 12 and 24 h, depending on the degree of pore opening. The final anodisation of the prestructured aluminium metal base under identical conditions (see Table 2) was followed again by detachment of the formed membrane from the aluminium metal base through the voltage reversal technique.

Table 2. Experimental conditions for aluminium anodisation leading to PAOX membranes with hexagonal pore geometry.

Electrolyte	Concentration [wt.-%]	Anodisation voltage [V]; time	Temperature [°C]
H_2SO_4	10	(25)[a]; 15–30	(5); 10–25
$H_2C_2O_4$	4	(40, 50); 30–60	(5); 0–25

[a] Number in parentheses: this work; others: possible temperature window which can be also used to form PAOX membranes under otherwise same conditions.

Dissolution of the Barrier Layer: To open the backside of the PAOX membrane the barrier layer was treated with a 5% phosphoric acid solution at 30 °C. Therefore the membrane was placed with the barrier layer face down on the phosphoric acid solution (see Table 1 for time intervals). After the time necessary for dissolution of the backside PAOX membrane it was carefully lifted off the acid bath, rinsed with distilled water for 30 min and thereafter washed with acetone.

Acknowledgments

We thank AMAG, Ranshofen, Austria for donation of the PURALUX aluminium metal sheets. Use of the SEM facility in the Dep. of Geology (Prof. Piller), Karl-Franzens-University Graz, Austria, is also acknowledged with gratitude.

[1] a) H. Masuda, K. Fukuda, *Science* **1995**, *268*, 1466; b) H. Masuda, H. Asoh, M. W. Watanabe, K. Nishio, M. Nakao, T. Tamamura, *Adv. Mater.* **2001**, *13*, 189; c) G. D. Sulka, S. Stroobants, V. Moshchalkov, G. Borghs, J. Celis, *J. Electrochem. Soc.* **2002**, *149*, D97; d) C. H. Martin, *Science* **1996**, *8*, 1739; e) M. Kang, S. Yu, N. Li, C. R. Martin, *Small* **2005**, *1*, 1–4; f) J. Yan, G. V. Rama Rao, M. Barela, D. A. Brevnov, Y. Jiang, H. Xu, G. P. López, P. B. Atanassov, *Adv. Mater.* **2003**, *15*, 2015–2018.
[2] See for example: a) J. Li, C. Papadopoulos, J. Xu, M. Moskovits, *Appl. Phys. Lett.* **1999**, *75*, 367; b) G. L. Hornyak, A. C. Dillon, P. A. Parilla, K. M. Jones, F. S. Fasoon, M. J. Heben, J. J. Schneider, N. Czap, *Nanostruct. Mater.* **1999**, *12*, 83; c) H. Masuda, M. Ohya, H. Asoh, M. Nohtomi, T. Tamamura, *Jpn. J. Appl. Phys.* **1999**, *38*, L1403; d) G. L. Hornyak, M. Kröll, R. Pugin, T. Sawitowski, G. Schmid, J.-O. Bovin, G. Karsson, H. Hofmeister, S. Hopfe, *Chem. Eur. J.* **1997**, *3*, 1951.
[3] T. Yanagishita, M. Sasaki, K. Nishio, H. Masuda, *Adv. Mater.* **2004**, *16*, 429–432.
[4] A. H. Greiner, J. H. Wendorf, M. Steinhart, *Nachr. Chem.* **2004**, *52*, 426.
[5] H.-P. Kormann, G. Schmid, K. Pelzer, K. Philippot, B. Chaudret, *Z. Anorg. Allg. Chem.* **2004**, *630*, 1913.
[6] J. P. O'Sullivan, G. C. Wood, *Proc. R. Soc.* **1970**, *A317*, 511.
[7] a) S. Ono, N. Masuko, *Corros. Sci.* **1992**, *33*, 503; b) S. Ono, H. Ichinose, N. Masuko, *Corros. Sci.* **1992**, *33*, 841; c) H. Uchi, T. Kanno, R. S. Alwitt, *J. Electrochem. Soc.* **2001**, *148*, B17–B23.
[8] H. Hu, in: *Metals Handbook*, 9th ed., American Society for Metals, Metals Park, OH, **1985**, vol. 9, pp. 692–699.
[9] D. Altenpohl, *Aluminium*, 4th ed., Aluminium-Verlag, Düsseldorf, **1979**, ch. 10, pp. 122–137.
[10] F. Li, L. Zhang, R. M. Metzger, *Chem. Mater.* **1998**, *10*, 2470.
[11] I. H. Yuan, F. Y. He, D. E. Sun, X. H. Xia, *Chem. Mater.* **2004**, *16*, 1841.
[12] T. Kyotani, W. H. Xu, Y. Yokoyama, J. Inahara, H. Touhara, A. Tomita, *J. Membr. Sci.* **2002**, *196*, 231–239.
[13] Y. C. Sui, B. Z. Cui, L. Martínez, R. Perez, D. J. Sellmyer, *Thin Solid Films* **2002**, *406*, 64–69.
[14] J. Randon, P. P. Mardilovich, A. N. Govyadinov, R. Paterson, *J. Colloid Interface Sci.* **1995**, *169*, 335.
[15] A. P. Li, F. Müller, A. Birner, K. Nielsch, U. Gösele, *J. Vac. Sci. Technol. A* **1999**, *17*, 1428.
[16] H. Masuda, H. Yamada, M. Satoh, H. Asoh, M. Nakao, T. Tamamura, *Appl. Phys. Lett.* **1997**, *71*, 2770.
[17] T. Xu, G. Zangari, R. M. Metzger, *Nano Lett.* **2002**, *2*, 37–41.
Received: December 22, 2004

